

Perched groundwater at the northwestern coast of Egypt: a case study of the Fuka Basin

Mohamed Yousif · Olaf Bubenzer

Received: 13 February 2011 / Accepted: 18 December 2011 / Published online: 4 January 2012
© The Author(s) 2012. This article is published with open access at Springerlink.com

Abstract Perched groundwater resources on the northwestern coast of Egypt have thus far been little studied. However, if replenished by rainwater, they can provide a considerable amount of renewable water, i.e., for sustainable irrigation. These resources are limited, show different salinity contents and are endangered by overuse, pollution and by the sea level rising in the context of global warming. This paper presents new climatic data, geomorphologic, geologic, geochemical and hydrological researches in combination with remote sensing and GIS applications from Fuka Basin. Fuka constitutes a special synclinal basin where the interbedded limestone and clays have been folded into gentle synclinal structures. Fractured Middle Miocene limestone represents the bearing formation for the perched groundwater. According to the hydrogeochemical analysis and the PHREEQC model, the aquifer is recharged during the winter season by rainwater from the surrounding tableland and the chemical evolution of the perched water is attributed to water–rock interaction and mixing of fresh water with sea water. The salinity of the perched water ranges from 2,126 to 2,644 mg/L whereas for the deep groundwater it reaches 9,800 mg/L. The study explores origin and potential of the perched groundwater of Fuka Basin and gives recommendations for a future sustainable use and further investigations.

Keywords Fuka Basin (Egypt) · Perched groundwater · Groundwater recharge · Rainfall/runoff · Hydrochemistry

Introduction

The hydrogeological framework of Egypt is composed of several different aquifer systems. They differ in general characteristics, including extension, transmissivity, renewability etc. (Hefny et al. 1992). Along the Mediterranean coast, the fractured limestone aquifer systems of Middle Miocene rocks can be found in the littoral zones. Here, groundwater generally occurs under phreatic conditions in the form of thin lenses floating over saline water and recharged from rainwater. Specific conditions for the presence of a water table known as perched groundwater in this aquifer exist in the Fuka Basin at the northwestern coast of Egypt. Perched aquifers occur when groundwater collects above a low-permeability layer of rock or sediment above the main water table. Perched water may be defined as a saturated zone that is above or not directly connected to the static water table (Freeze and Cherry 1979). In other regions of the world, perched groundwater is also recorded, e.g., in Jordan in Biyar El Ghussein (Kimberley and Abu-Jaber 2005), in France in the Vosges Mountains (Sailhac et al. 2009), and in Nevada, USA, at Yucca Mountain (Wu et al. 1999).

Until today, the hydrogeological situation of the Fuka Basin has only been little studied and is therefore not fully understood. During World War II, the British Army used dowsing to locate groundwater supplies (Moseley 1973). Geologists assisted Royal Engineers well-drilling units in the installation and development of shallow wells that yielded up to 23 m³/h from 0.25 m diameter holes (Rose 2004). Robins and Rose (2009) dated all British military

M. Yousif (✉)
Geology Department, Desert Research Center,
P.O.B. 11753, El Matriya, Cairo, Egypt
e-mail: yousif_mohamed80@daad-alumni.de

O. Bubenzer
Institute of Geography, Heidelberg University,
Im Neuenheimer Feld 348, 69120 Heidelberg, Germany
e-mail: olaf.bubenzer@geog.uni-heidelberg.de

geological activities in North Africa and the Middle East. They mentioned the work of Shotton (1944), who yielded new information about ‘desert’ hydrogeology based on borehole data. Along the Libyan and Egyptian Mediterranean coast, he observed perched groundwater with lower salt contents than in the main aquifer below. In the Fuka Basin, he identified an elongated syncline in which saturated limestone was underlain by clay. By drilling 61 boreholes, the resource became a valuable supply to the British Army, providing about 115 m³ of water per day.

El-Raey (1998) mentioned that underground water can also be found in the limestone layers below the Fuka Basin. They can produce water with an average quality at a rate of 20 m³/h. These data demonstrate the great importance of the groundwater for the basin. Underwood and Guth (1998) stated that perched water is able to supplement the groundwater supply and that the search for it led to the innovative use of the electrical resistivity method. This method was particularly successful in locating the depth of shallow limestone–clay contacts, the most favorable trap for perched water.

The main objectives of the present study are to examine and discuss the factors which generate the perched groundwater aquifer in the Fuka Basin, as an example but also for comparable aquifers in general. The study aims to give some indications of the importance of these aquifers, especially the fact that they contain renewable water of relatively low salinity and can therefore provide sustainable water, e.g., for agricultural uses. Another objective is to draw attention to the protection of such aquifers, which are highly vulnerable to overuse or effects of climatic changes like sea level rise. In this context, we carried out different investigations to clarify the nature of the perched aquifer in the Fuka Basin.

Materials and methods

The present work includes a group of studies which deal with geomorphology, geology, hydrogeology, hydrogeochemistry, remote sensing and the application of geographical information systems (GIS). The field studies comprised geomorphologic and geological mapping, surveying of water points, and the collection of groundwater samples and core samples from recently drilled wells. Some wells were drilled during field work (August 2009). The hydrogeologic data were obtained and measured during the field trip (such as; depth to water, total depth, water-bearing formations and hydro-geomorphologic units). Topographic maps with different scales and the geologic map were used during field investigations to demarcate the main landforms and structural elements with their relevancy for groundwater occurrence. A total of five groundwater samples and

two samples of rainfall and sea water were analyzed in the central laboratory of Desert Research Center (DRC) according to methods of the American Society of Testing and Materials (ASTM) (2002). Carbonate, bicarbonate, chloride, calcium and magnesium ions were determined volumetrically, while sodium and potassium were measured by flame photometer, and sulphate was measured by UV/V spectrophotometer. The hydrogen number (pH) and electrical conductivity (EC) of water samples were measured by pH and EC meter, respectively. The obtained data represent the main input to the PHREEQC model (Parkhurst and Appelo 1999, USGS), in order to discuss water–rock interactions. PHREEQC is a computer program (the model was used through AQUACHEM software version 3.7) that was designed to perform a variety of geochemical calculations based on ions association. GeoCover Landsat image mosaics (2000), obtained from NASA as compressed color imagery in MrSID TM file format (resolution 14.25 m, <https://zulu.ssc.nasa.gov/mrsid/mrsid.pl>), were used in addition to the geologic map (1:500,000, Conoco 1986) and field investigations to identify the geology of the study area. Data from the Shuttle Radar Topography Mission (SRTM, 90 m, <http://seamless.usgs.gov>), launched in February 2000, were used along with the ASTER Global Digital Elevation Model (ASTER GDEM, 28.5 m, <http://asterweb.jpl.nasa.gov/gdem-wist.asp>) to create a mosaic Digital Elevation Model (DEM) for the whole northwestern coast of Egypt (compare e.g., Bubenzer and Bolten 2008). DEM and Landsat images were first reprojected and subset to the study area in ERDAS IMAGINE (ver. 9.3), then imported into the ESRI ArcMap GIS software package (ver. 9.3). Since the spatial distribution of groundwater depends on the geomorphic and hydrological characteristics of the area, we used an indirect approach of hydro-geomorphological investigation. The ASTER GDEM was used within Arc Hydro (Maidment 2002) to produce multi-hydro layers such as drainage channels, catchment areas and stream orders, which were useful in the discussion of surface runoff and its relation to the groundwater recharge. All subsequent analyses and generation of maps were performed in ArcMap, ArcScene and Surfer software. The hydrogeological cross sections were generated by combining subsurface data provided from the wells’ lithology and surface geology with the assistance of Global Mapper software. These cross sections provided results clarifying the mechanisms of recharge and the factors which control groundwater occurrence.

Area of study

The northern sections of the Western Desert along the Mediterranean coast constitute the so-called northwestern

coastal zone (Fig. 1), which extends from Alexandria in the east for 520 km to El-Salloum on the Libyan border in the west and represents a portion of the small semi-arid belt of North Africa which receives winter rainfall. The zone varies in average width between 30 and 50 km and overlaps with the limestone plateau of the Western Desert in the south. The narrow low-lying coastal strip or northwestern coastal plain is delimited in the south by the escarpment of the Middle Miocene Marmarica tableland. Due to the irregularities of both the coastline and the tableland escarpment, the width of the coastal plain varies greatly from a few meters where the escarpment overlooks the Mediterranean Sea in the form of headlands, as in the case of the promontory of Ras El Hekma, to several kilometers, as in the case of the Fuka Basin in the middle part of the plain, where the escarpment of the tableland recedes southwards in a curved shape. Fuka Basin, located about 80 km east of Matrouh, extends over an area of about 370 km² and stretches along the coast for 29 km (Fig. 1). The area is bounded in the south and west by an

escarpment which rises 30–40 m above the plain and is dissected by a number of dry consequent valleys which either end in internal depressions or lead directly into the sea.

Climate

The northwestern coastal zone belongs to the subtropical Mediterranean climate with mild and wet winters and hot and dry summers. Matrouh receives winter rains, with an annual precipitation amount of 155 mm on average. In comparison, the annual evaporation rate is 1,578 mm (Ali et al. 2007, Table 1). Since the year 1998, the Desert Research Center has installed a weather station in Ras El Hekma (10 km to the west of the study area). From 1998 to 2006 the average annual precipitation was 101.5 mm (Table 2, Desert Research Center); this rainfall occurs mainly in winter season (from December to March) which is considered the wet season in the study area. The rainfalls represent the main source for the recharge of the perched groundwater.

Geomorphology

Regionally, the northwestern Mediterranean coastal zone, which extends between Alexandria and El Salloum, occupies the northern periphery of the great Marmarican Homoclinal plateau, which covers much of the Western Desert between the Qattara Depression and the Mediterranean Sea (Shata 1957). In general, it is distinguished into two main distinct physiographic features, the northern coastal plain and the southern tableland (Fig. 2).

The field work results of this study show that the present day landforms reflect the combined influence of several endogenetic and exogenetic factors, e.g., geologic structures, lithologic features, climatic conditions, and paleogeographic elements. These landforms include tableland, ridges, depressions, dunes and drainage channels. The geomorphologic setting influences the groundwater conditions of the study area and strongly controls the spreading of the surface runoff, which either accumulates in the depressions or drains into the sea. The following geomorphologic units can be distinguished (Fig. 2).

The coastal plain

The coastal plain occupies a narrow strip of land stretching along the Mediterranean Sea. Its maximum extent inland attains about 4.5 km. The coastal plain displays different landforms, which are influenced by the local geological structures. Generally, it slopes northward and has elevations from 10 to 40 m above sea level. It comprises elongated ridges, shallow depressions and dunes. The ridges

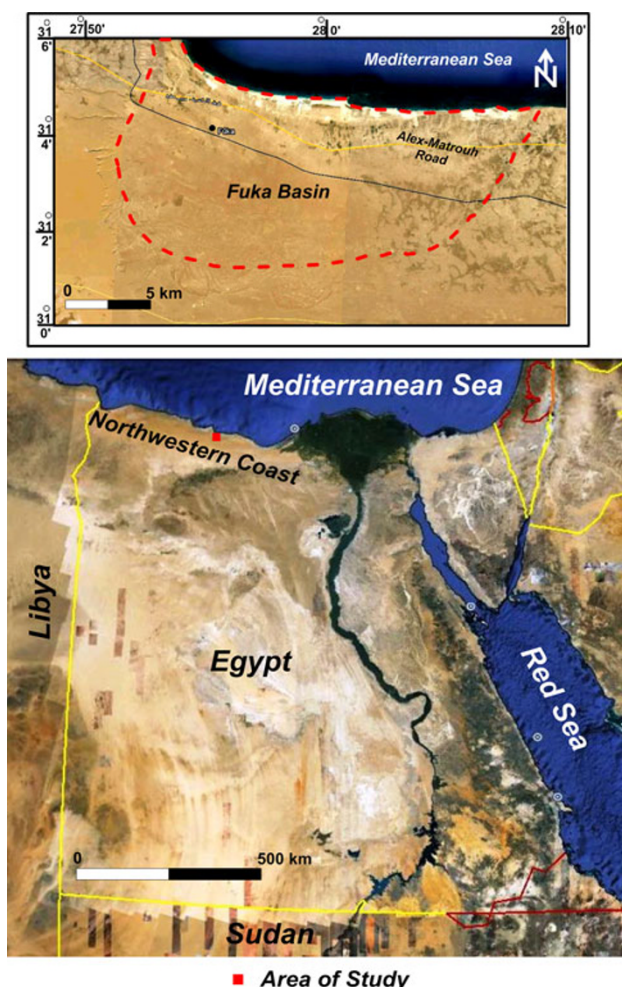


Fig. 1 Location map of the study area. [Google earth TM 2009]

Table 1 Main climatic data (1945–1992) at Matrouh Station in northwestern coast of Egypt (Ali et al. 2007)

Climatic parameters	Jan.	Feb.	Mar.	Apr.	May	Jun.	Jul.	Aug.	Sep.	Oct.	Nov.	Dec.	Annual
Rainfall (mm)	36.8	21.3	12	3.8	2.7	1.1	0	0.5	1.5	16.1	23.6	36	<i>155.4</i>
Temp. (max.) (°C)	18	18.8	20.2	22.6	25.5	27.7	29.1	29.8	28.6	27	23.3	19.6	24.2
Temp. (min.) (°C)	8	8.3	9.6	11.7	14.5	18.1	20.1	21	19.6	16.7	13.2	10	14.2
Evaporation (mm)	90	85	115	145	160	158	180	175	150	130	100	90	<i>1,578</i>
Radiation (cal cm ⁻² day ⁻¹)	233	319	429	538	574	590	594	553	462	343	243	232	426
Wind speed (m s ⁻¹)	8.8	6.5	6.3	6.3	5.6	5.4	5.9	5.2	4.9	4.5	4.8	6.1	

In the annual column: the italicized values show annual total and the others are the annual average

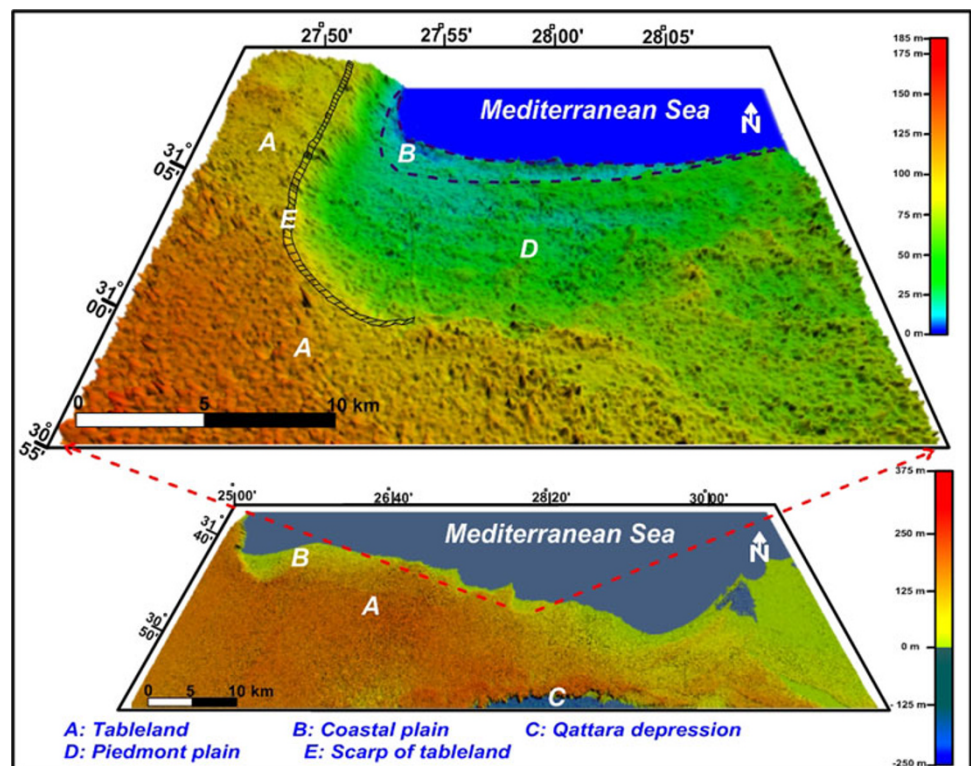
Matrouh City is 80 km to the west of the study area

Table 2 Monthly rainfall data in Ras El Hekma Station (1998–2006)

Season	Months							Total (mm)	Average (mm)
	Oct.	Nov.	Dec.	Jan.	Feb.	Mar.	Apr.		
1998–1999	0	5.2	51.8	20.55	20	0.4	0	97.95	101.5
1999–2000	17.7	6.8	1.5	93.92	7	12.4	2	141.32	
2000–2001	27.5	17.6	42.8	2.3	3.9	0	0	94.1	
2001–2002	0	0	7.85	32.7	2.8	0	0	43.35	
2002–2003	0	0	4.2	40	30.8	34	0	109	
2003–2004	0	14.5	36.5	33.5	6.5	0	0	91	
2004–2005	17.4	25.4	42.7	36.5	0	0	0	122	
2005–2006	7.6	32.9	34.2	33.5	5	0	0	113.2	

No rainfall is recorded in other months

Ras El Hekma station is 10 km to the west of the study area

Fig. 2 Digital elevation modeling (DEM) of the northwestern coast and Fuka Basin showing the main landforms

stretch parallel to the coast line. They mark the ancient high stand of the Mediterranean Sea. The first ridge consists of friable, highly porous oolitic limestone, has an elevation from 30 m in the west to 15 m in the east and a length of 17 km. The second and third ridges consist of cemented oolitic limestone and have lengths of 16 and 4 km and heights of 36–40 m. Depressions are situated between the first and the second ridge. They have elevations of 10 m above sea level and cover an area of about 5 km². With regard to the hydrographic response of the elongated ridges, the one closest to shore with its cover of loose sand acts as collecting shed area, through which most of the region's infiltration occurs.

The piedmont plain

The piedmont plain extends to the south of the coastal plain and forms a transition zone between the tableland and the coastal plain. It has a width of 24 km, a length of 7 km and covers an area of 145 km². The plain contains inland ridges with elevations of 35, 40 and 45 m above sea level. These ridges are separated by depressions. In addition, dunes and salt marshes are recorded in a few spots inside the plain. Most of the drained surface runoff from the tableland is directed to the north toward the piedmont and/or the coastal plain.

The tableland

The tableland reaches a maximum elevation of 170 m above sea level (the scarp at 90–100 m and the main parts at 110–135 m above sea level). It is dominated by hard limestone strata developed into a flat to slightly undulated plain, at several localities revealing closed to sub-closed hollows into which loamy deposits are accumulated. The tableland is bounded by an escarpment facing the piedmont plain. This geomorphic unit represents the principal watershed area and its surface slopes northward and eastward. Consequently, the surface runoff is directed into the basin and hence recharges the perched groundwater. The limestone of the tableland is also fractured, which plays an important role for the recharge of the groundwater.

Geology

The exposed outcrop in the study area is composed of Late Tertiary (Neogene rocks) and Quaternary sediments. They exhibit various lithotypes which reflect different paleogeographic, paleoclimatic, and paleotectonic conditions. The geologic succession in Fuka Basin and its surrounding catchment area will be discussed according to the geologic map of Conoco, 1986 (Fig. 3a) and our field investigations. Two modifications to the geologic map were made on the

basis of our studies. The first one is the completion of two ridges (Pleistocene) inside the Fuka Basin. These ridges are confirmed by the Landsat image (Fig. 3b) and the DEM. The second one is the addition of beach sand which was found along the coast during the field study. The geologic succession of Fuka Basin from base to top is presented in the following section

Middle Miocene rocks (Marmarica Formation)

The Marmarica Formation is made up of fissured, cavernous fossiliferous, limestone which is occasionally dolomitic and is intercalated with clay and marl. Hammad (1972) subdivided the Middle Miocene rocks into two zones forming the structural plateau. The first includes chalky, marly, fossiliferous and sandy limestone, and the second comprises shale and clay beds intercalated with limestone has the same characteristics of the first zone. The Middle Miocene fissured limestone is considered the sole aquifer in the study area containing groundwater under perched conditions.

Pliocene rocks (El Hagif Formation)

Pliocene rocks are not as common as the other deposits in the area. They are recorded outside of the study area, i.e., to the south and west of Fuka Basin, where they overlay the Middle Miocene rocks. These rocks consist mainly of limestone interbedded with marl and clay.

Pleistocene limestones (Alexandria Formation)

Pleistocene deposits are present at the surface along the coast and on the basin floor in the form of ridges consisting of oolitic limestone. This limestone is white in color, darkening and hardening with age. It is composed of oolitic grains, mixed with quartz sands, shell fragments and foraminiferal tests, and cemented by calcium carbonate. Some of the limestone has a well-defined jointing pattern. In some areas, it is exposed above sea level, but it can also be encountered in the subsurface. Here, it was detected in all the drilled wells in the study area as a thick layer overlying the Miocene clay beds.

Pleistocene and Holocene alluvial deposits

Alluvial deposits are widely distributed in the area of study and cover the floor of Fuka Basin and the lower parts of the drainage channels, where they are composed of calcareous mudstone (silt and clay) mixed with minor gravels delivered by the runoff water from the Middle Miocene exposures. On the other hand, the alluvial deposits which are located on the floor of the basin are composed of

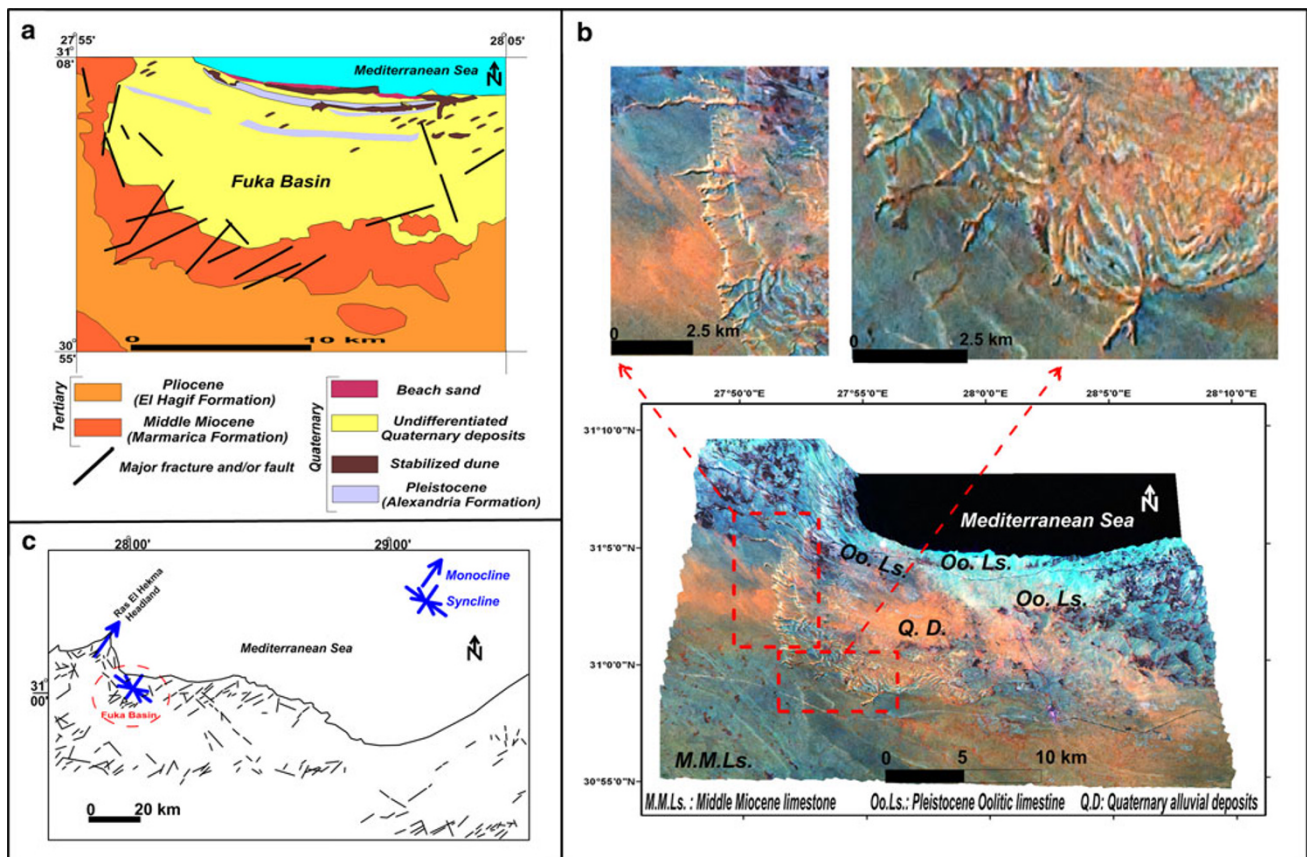


Fig. 3 Geology and structural settings of Fuka Basin. **a** Geologic map of Fuka Basin, modified after Conoco (1986). The modification in the map includes the addition of the beach sand and the inland ridges. **b** Geo Coverage landsat ETM (2000) overlay DEM showing

the main rock units in the study area. The *upper part* of the figure shows two groups of draining basins which flow from west to east and from south to north. **c** Structural lineaments for a part of the northwestern coast of Egypt, from Conoco (1986)

calcareous materials formed of oolitic sand and shell fragments together with organic matter, quartz and clays.

Holocene

The Holocene deposits in the study area are dominated by oolitic sand dunes. These dunes are developed in series either along the Mediterranean coast or inland. They trend in an almost E–W direction, sub-parallel to the shore line, and are free or stationary, resting irregularly above the Pleistocene limestone (ridges). They are composed of oolitic sand, shell fragments, echinoid spines and quartz grains and are derived from the Pleistocene and Miocene sediments.

Structural setting

In general, the northwestern coast of Egypt represents a zone of the mobile shelf of Egypt (Said 1990). The sedimentary cover of this portion displays numerous landforms produced by tensional and compressional forces. The Middle Miocene homoclinal plateau (part of the tableland)

is the most prominent structural feature. The northern extreme of the homoclinal plateau is affected by a number of monoclinical structures, dipping in a NE–SW direction. These monoclines have been detected in some localities along the coast in the form of heads extending into the sea. To the west of the Fuka Basin, Ras El Hekma, with a NE–SE orientation, is one example of these monoclines. According to Shata (1955), they were developed toward the Middle Miocene times. Fuka Basin is thought to be a synclinal structure which has specific lithologic conditions favoring the development of perched groundwater. The structural setting is the main factor which controls the groundwater occurrence. Limestone and clay interbeds of the Marmarica Formation were folded, forming a synclinal basin and keeping the perched water above the main saline water table. The clay band separates the perched water and the underlying saline water. Due to epirogenesis, the Ras El Hekma headland created numerous lines of weakness. The fracture systems are well pronounced around Fuka Basin and are responsible for the development of the drainage channels (Fig. 3b, c). These drainage channels control to a great extent the surface runoff into Fuka Basin. Around

Fuka Basin, steep escarpments have been initiated locally by faults at the edge of the tableland with strikes of NE–SW and W–E (Fig. 3c).

Results and discussion

Hydrogeology

The variations in the physiographic, geologic and climatic factors cause significant differences in the groundwater conditions of the Fuka Basin. The Middle Miocene Marmarica Formation, which forms the country rocks of the study area, is composed of limestone with clay intercalations. Structurally, small-scale homoclinal and synclinal folding and fissuring are the most common features. Such conditions cause groundwater to occur as separated sheets that accumulate in the porous limestone above the clay contacts.

Regional rainfall is thought to be the only source of water supporting the perched water table by surface runoff and infiltration. As a result, the salinity of the water in the structural basin should be lower than that of the main water table of the Middle Miocene aquifer. In the tableland, for example, a well with a total depth of 126 m was drilled. It reaches a depth of 2 m below the sea level and its water shows a salinity of 9,800 mg/L (total dissolved solids). On the other hand, the perched water table in the Fuka Basin ranges between 10 m below and 3.6 m above sea level and has salinity values between 2,126 and 2,644 mg/L (Table 3).

The depth to the water table in the Fuka structural basin varies according to the topography and the depth to the subsurface confining layers. Five new wells in the study area, which tapped the perched aquifer, were encountered in the present study (Fig. 4; Tables 3, 4). The subsurface lithology of these wells was obtained from the core samples; some wells that yielded water in the past are dry today as a result of overpumping. Other wells have been destroyed. FAO (1970) mentioned six drilled wells tapping the limestone aquifer in Fuka. All of them were originally

equipped with turbine pumps but in March 1968 only three of them were operating. The pumps are capable of retrieving about 25 m³/h, but in 2009 no more than two were working simultaneously and they were operated no more than 4 h/day during the irrigation season from October to February. During the non-irrigation season, the pumps are operated much less as they only supply water for Fuka village. The total annual withdrawal is estimated to be about 48,000 m³ but in some years the pumping is much greater. El-Sharabi (2000) measured one well in Fuka where the water table is 8.75 m above sea level and found a salinity of 2,694 mg/L. Mudallal (1990) reported seven drilled wells, five of which were drilled in 1984 and two of which in 1989. They substituted older ones and reach a total depth of between 30 and 40 m. The static water level varies between 17.5 and 18.6 m below the ground surface and the dynamic water level ranges from 18.8 to 23.8 m. The total dissolved solids for the water of these wells range between 2,000 and 2,700 mg/L. However, they produce between 125 and 150 m³/h, which is about half the proven quantity of the whole basin and is sufficient for the total number demand (Mudallal 1990). Some of these wells were dry in 2009 because they are located about 180 m outside of the basin. This suggests that the groundwater in the Fuka Basin is restricted to the basin itself.

The subsurface lithologic data from the studied wells were used in combination with surface geologic and DEM data for the drawing of hydrogeologic cross sections (Fig. 5). The claystone layer underneath the water-bearing fractured limestone acts as a barrier for groundwater. It is of variable thickness, for example it is 12 m thick in well no. 1, 2 m thick in well no. 2 and 10 m thick in well no. 5. The other two wells did not penetrate the claystone layer. Based on these results, it appears that this layer is interbedded with the Middle Miocene limestone as a lens. Shaaban (2001) did a geophysical study of an area in the southeastern part of Fuka Basin. He detected a deep aquifer of Miocene age below a thick clay cap at depths ranging from >50 to >160 m below ground surface. Its lithology comprises sandy limestone interbedded with sandstone and siltstone. The groundwater in this aquifer is confined by the

Table 3 Hydrogeological data of the wells tapping the perched aquifer in Fuka Basin

Aquifer	Well no.	Long. east	Lat. north	Total depth (M)	Depth to water from ground (M)	Ground elevation from sea level (M)	Depth to water from sea level (M)	TDS (mg/L)	Water-bearing bed	Geomorphologic unit
Middle Miocene	1	27°55'06"	31°04'05"	32	28	22.2	−5.8	2126	Fractured limestone	Depression
	2	27°55'09"	31°04'05"	24	20	19.4	−0.6	2283		
	3	27°54'39"	31°04'30"	25	18	21.6	3.6	2498		
	4	27°54'36"	31°04'32"	25	18	20.3	2.3	2644		
	5	27°54'28"	31°04'37"	42	30	20	−10	2384		

Wells location: see Fig. 7

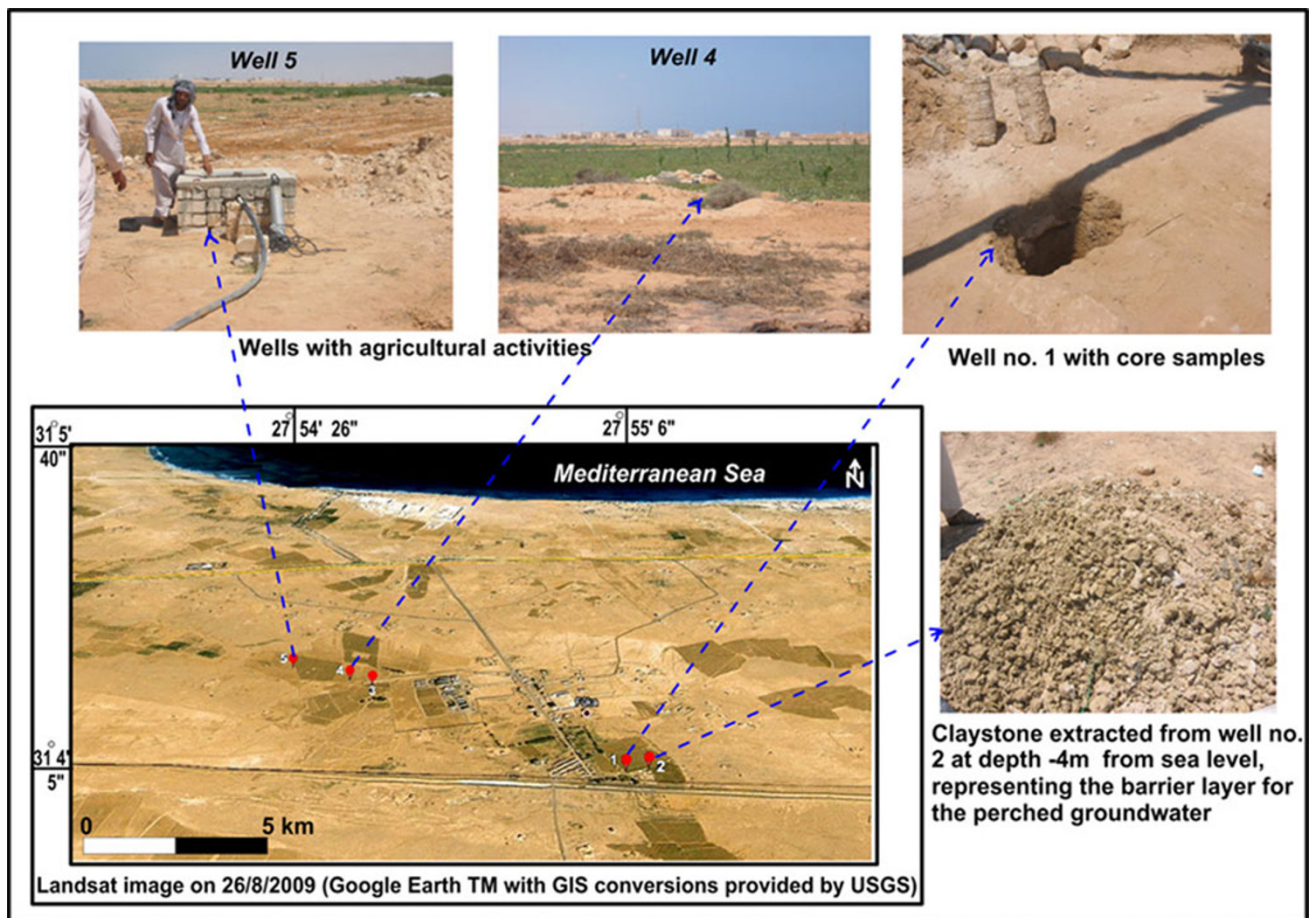


Fig. 4 Wells location map of Fuka Basin with some field photos

overlying thick clay zone. The aquifer resistivity suggests saline water conditions due to seawater intrusion from the Mediterranean.

In addition, the hydrogeologic cross sections show that two faults may accompany the folding structure and act as a conduit for groundwater (Fig. 5). We conclude that such basins are recharged by rainfall, which percolates through less thicker limestones, and that consequently the salinity of the water contained under perched conditions will be lower than that of the underlying main saline water table.

Hydro-physiography, drainage pattern and surface runoff

The northwestern Mediterranean coastal zone can be differentiated into two main physiographic provinces: the elevated tableland in the south and the coastal zone to the north. A great number of drainage channels dissect the tableland, the major watershed area. They are structurally controlled and well developed in areas where lineaments of weakness are common (Fig. 3b, c). Rainwater flows to the north and partially toward the east to the study

area, following the regional slope of the surface. The study area is covered by an intensive drainage network (Fig. 6). A portion of the rainwater probably infiltrates through joints and fractures into the lower limestone aquifers. However, the presence of a thin hard crust accelerates surface runoff toward the Fuka Basin. In addition, the coastal ridges lead to the conservation of soil water and surface water. The elongated depressions in the basin also act as collecting micro-basins for the runoff water. FAO (1970) estimated an annual runoff of $4 \times 10^5 \text{ m}^3$ for the northwestern coastal zone using cistern measurements. Sewidan (1978) estimated the water budget of several pilot areas on the northwestern coast of Egypt over 5 years. In these 5 years, he found that the total amount of rainfall reaching Fuka Basin (275 km^2) was 32.5 million m^3 , the average annual amount of surface runoff inflow was 3.8 million m^3 and the groundwater inflow was 0.067 million m^3 . On the other hand, Mudallal (1990) used FAO results and estimated the annual runoff in and around Fuka Basin for an area of 570 km^2 at about 2.2 million m^3/year , including wadi runoff and sheet runoff.

Table 4 The hydrochemical data of the perched groundwater in Fuka Basin

Aquifer	Well No.	EC $\mu\text{S/cm}$	pH	(TDS) (mg/L)	Units	Na^+	K^+	Ca^{2+}	Mg^{2+}	Sum. cat.	CO_3^{2-}	HCO_3^-	Cl^-	SO_4^{2-}	Sum. ani.	Water type	$\text{Ca}^{2+}/\text{Mg}^{2+}$ ratio
Middle Miocene fractured limestone	1	3,600	7.75	2,126	meq/L	18.91	0.7	8.15	8.3	36.06	0.2	5.8	18	12	36.00	Na-Cl	0.98
					e %	52.44	1.94	22.60	23.02		0.56	16.11	50.00	33.33			
	2	3,800	7.8	2,283	meq/L	19.2	1	8.5	10	38.70	0	7	19	12.95	38.95	Na-Cl	0.85
					e %	49.61	2.58	21.96	25.84		0.00	17.97	48.78	33.25			
	3	4,100	7.55	2,498	meq/L	30.25	1.14	2.5	7.5	41.39	0.4	8.8	17	15	41.20	Na-Cl	0.33
					e %	73.09	2.75	6.04	18.12		0.97	21.36	41.26	36.41			
	4	4,300	7.6	2,644	meq/L	31.5	1.5	2.9	8	43.90	0	9.5	18.5	15.8	43.80	Na-Cl	0.36
					e %	71.75	3.42	6.61	18.22		0.00	21.69	42.24	36.07			
	5	4,010	7.53	2,384	meq/L	26.75	1.19	3.5	8.75	40.19	0.6	9.5	17	13.2	40.30	Na-Cl	0.40
					e %	66.56	2.96	8.71	21.77		1.49	23.57	42.18	32.75			
Rainfall	R	610	6.1	327	meq/L	3.1	0.15	1.8	1.6	6.65	0.4	5	0.63	0.16	6.19	Na-HCO ₃	1.13
					e %	46.62	2.26	27.07	24.06		6.46	80.78	10.18	2.58			
Sea water	S	66,000	8.5	39,732	meq/L	522	11	20	116	669.00	0.333	2.5	642.5	54	699.33	Na-Cl	0.17
					e %	78.03	1.64	2.99	17.34		0.05	0.36	91.87	7.72			

Sum. cat. summation cations, Sum. ani. summation anions, TDS total dissolved salts

Implications of climatic changes and sea water rise for the studied aquifer

It is expected that climate change will take place during this century in spite of the international efforts to reduce greenhouse gas emissions (IPCC 2007). El-Raey et al. (1999) stated that natural sea level rise along the northern Egyptian coast is about 0.4 and 5 mm/year; while IPCC (2007) predicted that the sea level rise will be between 0.15 and 0.9 m until the year 2100. This change is expected to exacerbate the already existing environmental problems. In particular, coastal areas all over the world are expected to suffer from the impacts of sea level rise, i.e., from coastal erosion, subsidence, pollution, and land use changes.

In the study area, sea level rise will also affect the groundwater resources and the ecosystem, mainly by causing saline intrusions. This holds true for the perched groundwater as well as the main aquifer. Connections between sea level and the groundwater are modified by pumping and recharge activities. However, the impacts of the sea level rise on the groundwater resources via saline intrusion into coastal aquifers will vary considerably, depending on geography, topography, and the geologic and geomorphologic characteristics of the coastlines. On the basis of modeling studies, Sherif and Singh (1999) concluded that a 50 cm increase in sea level will cause an additional intrusion of saline water of some 9 km into the Nile Delta. On the other hand, the assumed increase in temperature and evaporation and the decrease in rainfall may lead to a reduction of the perched water recharge and therefore will create problems for agriculture.

Hydrogeochemistry

The chemistry of the groundwater is crucial for understanding the hydrogeological conditions of an aquifer. The present hydrogeological setting of the perched aquifer indicates that it behaves as an unconfined aquifer. The mean pH value of 7.6 of the studied samples greatly exceeds that of rainwater (pH 6.1, Table 4). This is a result of several chemical reactions within the unsaturated zone as well as a long residence time in the fissured limestone aquifer. The local precipitation is believed to be the dominant source of recharge. The total dissolved solids (TDS) of the studied groundwater vary between 2,126 and 2,644 mg/L, meaning that the perched groundwater is mainly brackish. The lithologic properties of the aquifer affect the type and concentration of the different dissolved solids (Table 4). The sequences of the ions show no variation in the chemical composition of the water, which is mainly controlled by the lithology of the recharging and the discharging area as well as the lithology of the water-bearing formation. The ion dominance in the studied

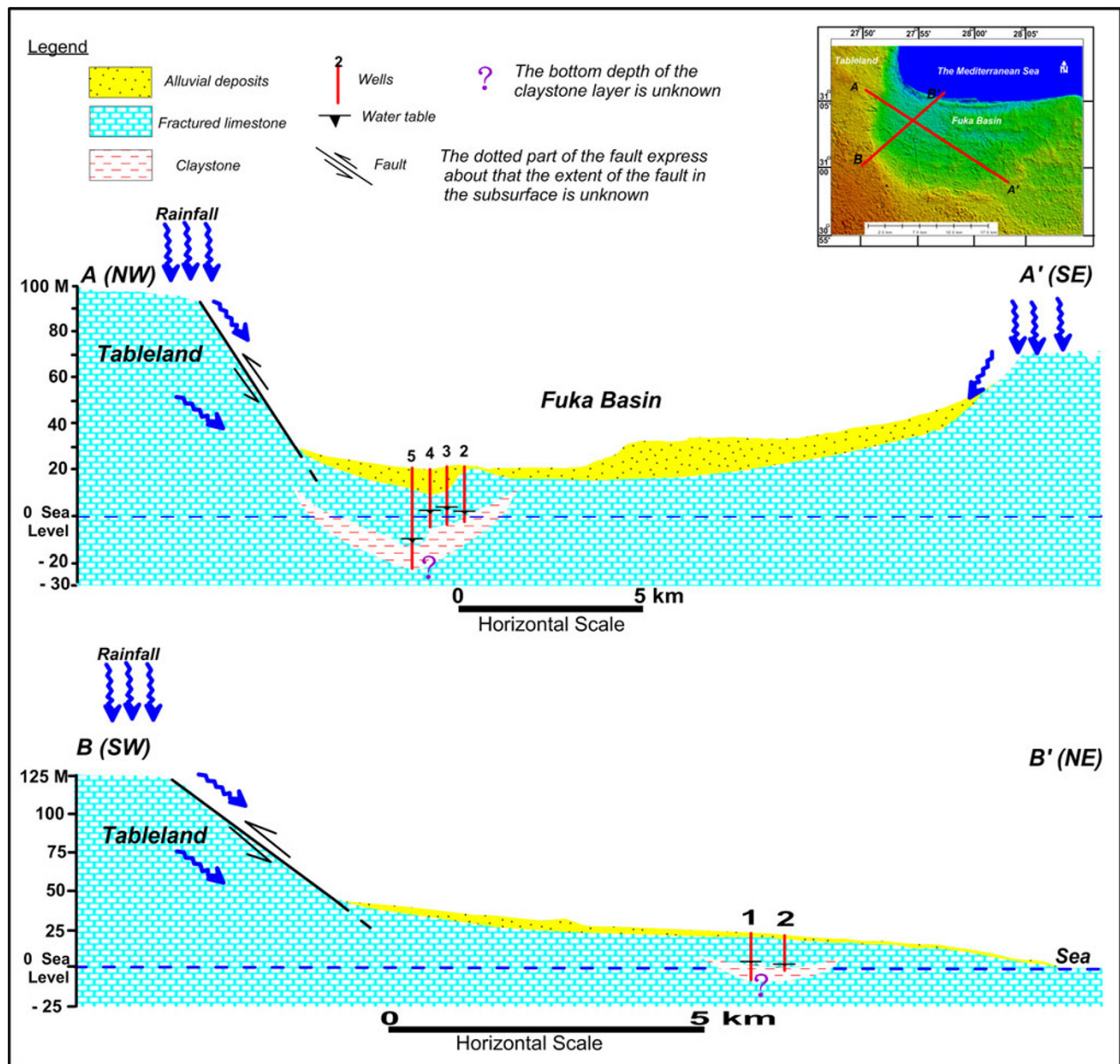


Fig. 5 Hydrogeological cross sections (A–A' and B–B') in Fuka Basin

groundwater follows the sequence $\text{Cl}^- > \text{SO}_4^{2-} > \text{HCO}_3^-$ and $\text{Na}^+ > \text{Mg}^{2+} > \text{Ca}^{2+}$. This chloride-sodium water type typically results from leaching and dissolution of terrestrial salts.

Genesis of groundwater

The Piper diagram (Piper 1944) constitutes a useful tool in the interpretation of water chemistry. The studied groundwater samples fall into the sub-area 7 of the Piper diagram, which means that the non-carbonate alkali exceeds 50% (Fig. 7a). The chemical properties of the

groundwater are dominated by alkalis and strong acids. The studied samples within sub-area 7 therefore demonstrate nearly marine conditions, where the marine deposits of the Middle Miocene limestone predominate. On the other hand, the local rainwater sample fall in sub-area 9 which is characterized by no one cation–anion pair exceeds 50%.

Scholler's diagram (Scholler 1962) was developed to enable a quick visual comparison of different water chemical composition. The relationship between two constituents (in milliequivalent per liter) of two different samples is comparatively expressed by the slopes of the straight lines connecting these constituents. Parallel lines in

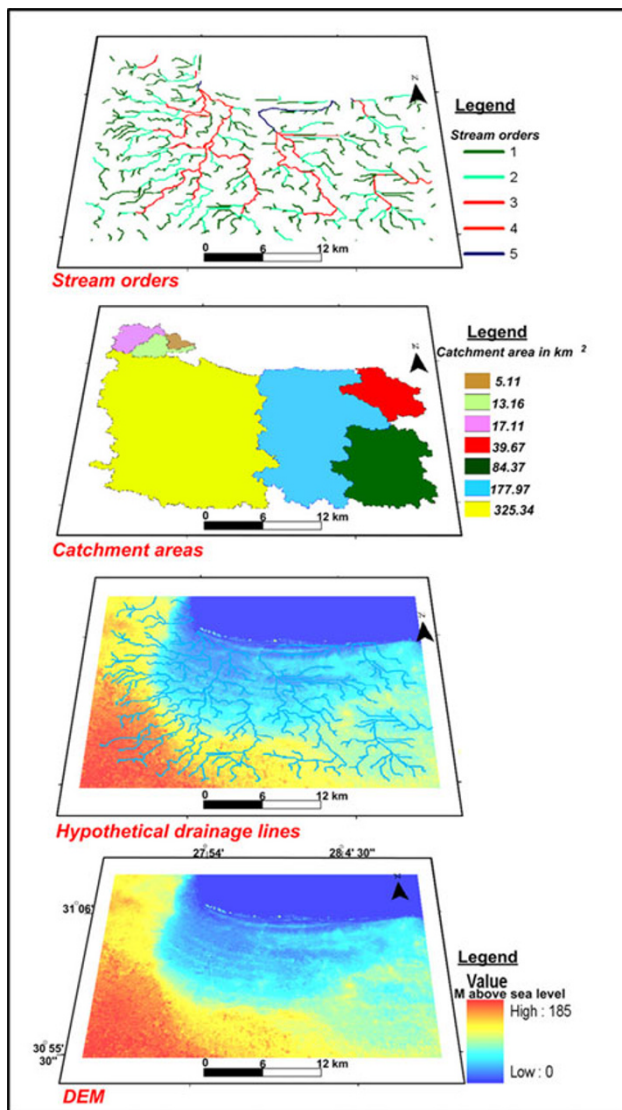


Fig. 6 Hydro-layers illustrate the intensive drainage network and catchment areas of Fuka basin, these layers are obtained from DEM using Arc Hydro software

the diagram express an identical relationship between the charged chemical species. After plotting each component of the chemical constitution of the studied groundwater samples, the main group can be distinguished into $\text{Na} + \text{K} > \text{Mg} > \text{Ca}$ and $\text{Cl} > \text{SO}_4 > \text{HCO}_3$, which reflects an advanced stage of hydrochemical evolution (Fig. 7b). The general shape of such groundwater profiles shows some similarity to rainwater, indicating that such groundwater is of meteoric origin and affected by continental processes.

Generally, Fig. 7a, b shows some resemblance between sea and rainwater with perched groundwater, this can be interpreted as the main source of the perched groundwater is the rainwater with the presence of interference from sea water.

Hypothetical salts

Hypothetically, the ions of the strong acids (Cl^- and SO_4^{2-}) form a chemical combination with alkalis (Na^+ and K^+) and the rest of the acid radicals combine with the alkaline earths (Ca^{2+} and Mg^{2+}) (Collins 1923; Zaporozec 1972). In the present study, the combination between major anions and cations reveals the formation of two main assemblages of hypothetical salts combinations in the perched groundwater of the Middle Miocene fractured limestone aquifer. The two recorded assemblages are:

1. NaCl , Na_2SO_4 , MgSO_4 , $\text{Mg}(\text{HCO}_3)_2$ and $\text{Ca}(\text{HCO}_3)_2$ in the wells no. 3, 4 and 5.
2. NaCl , Na_2SO_4 , MgSO_4 , CaSO_4 and $\text{Ca}(\text{HCO}_3)_2$ in the wells no. 1 and 2.

The recorded assemblages contain two bicarbonate salts which reflect the dilution effect of rainwater and draining of wadis on the groundwater. The chemical evolution starts with dominant HCO_3^- salts (assemblage 1) which change to dominant SO_4^{2-} salts (assemblage 2) at the end. The dominance of sulphate salts is mainly attributed to the leaching of the terrestrial salts. This group indicates the meteoric origin of the groundwater.

On the other hand, with regard to Table 4, there is an increase in the proportion of bicarbonate as well as the record of rare amount of carbonate where pH values range between 7.53 and 7.8. The carbonate ions in the study area are mainly derived from calcium carbonate rocks, where the solubility is low, but increases markedly in the presence of CO_2 , forming the highly soluble bicarbonates. This indicates that the amount of bicarbonate in solution is dependent on the amount of CO_2 in water, and in turn on its pressure in the atmosphere over water. The initial source of CO_2 is rainfall which subsequently dissolves carbonate ions. In addition, the biological activity in the soil and the chemical processes release considerable amounts of CO_2 which help in the contamination of groundwater to increase bicarbonate ions. Worsley (1939) stated that the addition of salts to water may cause reduction in its pH values depending on the quality and type of the added salts, whereas the leaching of salts may cause a rapid rise in the pH. The exchangeable cations like Ca^{2+} , Mg^{2+} , K^+ , Na^+ , and hydrogen affect markedly the water reaction. Na and K cations make water slightly more alkaline than do Ca^{2+} and Mg^{2+} . The presence of a considerable content of CaCO_3 increases the pH value of water, and raises the alkalinity (i.e., $\text{H}_2\text{O} + \text{CaCO}_3 \leftrightarrow \text{CO}_3^{2-} + \text{H}_2\text{O} + \text{Ca}^{2+}$). In addition, the pH value of the sea water sample is 8.5, consistent with the values recorded by Mohamed and Fahmy (2005) along the Mediterranean coast in the northwestern coast of Egypt where the lowest values of pH are (8.20 ± 0.04) .

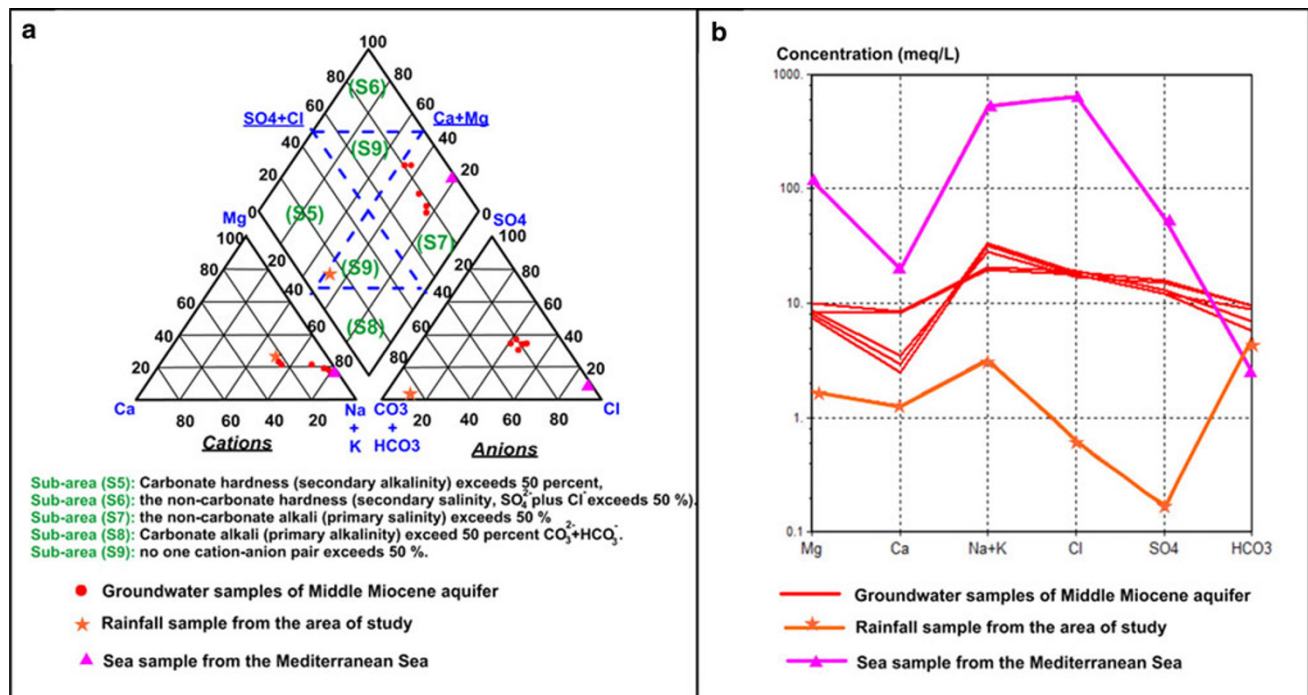


Fig. 7 Graphical representation of the geochemical data of the perched groundwater in Fuka Basin. **a** Piper diagram. **b** Schoeller diagram

Water–rock interaction

The water–rock interaction, the effect of solution and leaching processes on the mineralization of groundwater in the studied aquifer, was studied with the implementation of the PHREEQC model (follows the convention: saturation index = $\log [IAP/KT]$) and the recorded hypothetical salts (Table 5). Although the main source of the perched groundwater is the rainfall, it is clear that the increase of groundwater salinity is due to soluble salts in the water-bearing formation and the mixing with sea water. The data obtained from the PHREEQC model reveal that most groundwater samples are supersaturated with dolomite ($\text{CaMg}(\text{CO}_3)_2$), calcite and aragonite (CaCO_3). The Middle Miocene rocks are composed of 72–91% CaCO_3 , 4–7% MgCO_3 and 5–13% SiO_2 according to the rock chemical analysis carried out by Atwa (1979). One of the most important hydrochemical coefficients (ion ratios) is the calcium/magnesium ratio ($\text{Ca}^{2+}/\text{rMg}^{2+}$). All of the analyzed groundwater samples from the fissured limestone aquifer have an $\text{Ca}^{2+}/\text{Mg}^{2+}$ ratio less than unity, i.e., magnesium ions exceed calcium ions. The groundwater of this aquifer flows entirely through limestone-dolomite terrain. This is due to the precipitation of calcium carbonate or calcium sulfate in the fractures after long flow distances. The values of the $\text{Ca}^{2+}/\text{rMg}^{2+}$ ratio were calculated (meq/L concentration), they range from 0.3 to 0.9 with a mean value of 0.7. These values are above that of the seawater (0.17) but below that of the rainwater in the study

area (1.12). This is due to the presence of CaCO_3 and $\text{CaMg}(\text{CO}_3)_2$ materials, which is confirmed by the saturation indices of carbonate minerals in the groundwater samples of the fissured limestone aquifer. It seems reasonable that the sources of the magnesium leading to the increase of Mg^{2+} in the groundwater are the dolomitic limestone and dolomite which form the main rocks in the watershed area and water-bearing formation where these rocks are subjected to leaching and dissolution after rainfall which recharges the perched groundwater.

It can be concluded that, the perched aquifer is recharged by a mix of rainwater and intruding sea water, even if that intruding sea water is relict from a higher sea level stand or some sort of catastrophic storm surge. The depth to perched water in Fuka Basin is close to sea level and in some wells even below sea level where the distance from the drilled wells to the sea is about 10 km. Therefore, sea water intrusion can play a role in increasing magnesium percentages. The chemical evolution and the raise in TDS of the perched water than rainwater (as it appears in Fig. 7a, b) can be attributed to water–rock interaction and mixing of fresh and sea water.

Summary and conclusions

The main objectives of the present study are to monitor and discuss the factors leading to the occurrence of a perched groundwater aquifer in the Fuka Basin (370 km²) at the

Table 5 Saturation indices of the perched groundwater due to chemical equilibrium with Middle Miocene aquifer matrix (obtained from PHREEQC Model), Fuka Basin

Wells no.	Saturation mineral indices					
	Anhydrite	Aragonite	Calcite	Dolomite	Gypsum	Sulfur
1	−1.09	0.75	0.89	1.99	−0.87	−53.3
2	−1.47	0.19	0.34	1.24	−1.25	−51.58
3	−1.62	0.28	0.43	1.46	−1.4	−52.89
4	−1.4	0.23	0.37	1.27	−1.18	−51.04
5	−1.11	0.63	0.77	1.68	−0.89	−52.92

The input data of PHREEQC model is the data in Table 4

northwestern coast of Egypt. The study demonstrates the importance of this aquifer, which contains renewable water of relatively low salinity that is therefore usable for agricultural activities. To achieve these objectives, field investigations, laboratory and computer analyses were carried out. The field work included surveying of water points and core samples from recent drillings, the demarcation of the main landforms and the investigation of the structural setting with their implications for groundwater occurrences. DEM, Landsat images, topographic and geologic maps, chemical analysis, the application of GIS-software and a chemical model were used for data extraction and interpretation. The study area receives a yearly amount of rainfall averaging 101.5 mm, most likely the main source for recharging the perched groundwater. Fuka Basin is recharged by runoff or by subsurface inflow of rainwater. The subsurface lithologic data of the studied wells were combined with the surface geology and DEM for drawing hydrogeologic cross sections. These sections show that two faults may accompany the folding structure and act as a conduit for groundwater by downward processes. It can be concluded that the perched conditions are of intermittent and/or perennial nature depending on the activity of the replenishment processes. Therefore, the salinity of the water contained under perched conditions is lower than that of the underlying main saline water table. Sea level rise will have impacts on the groundwater resources and the ecosystem, mainly due to saline water intrusion. These correlations between sea level and groundwater are modified by pumping and recharge activities. Also, the impacts of sea level rise on groundwater resources via saline intrusion into coastal aquifers will vary considerably, depending on the topography. The salinity of perched water in Fuka Basin is lower than that of the main water table of the Middle Miocene aquifer. The TDS of the studied groundwater vary between 2,126 and 2,644 mg/L, meaning that the perched groundwater is mainly brackish. The chemical evolution and the raise in TDS of the perched water than rainwater can be attributed

to water–rock interaction and mixing of fresh and sea water.

In the future, the perched groundwater might be contaminated as a result of sea level rise, sea water intrusion and decrease of aquifer recharge. Hence, coastal protection and water management measures should be established. Furthermore, the pumping from the studied aquifer must be managed very carefully to preserve the depth of the perched groundwater. New wells should not be drilled to a depth below sea level. Otherwise, the sea water is expected to invade the perched groundwater. This holds true in particular for the low-lying areas of the basin. Consequently, the recommended area for future drillings is the southern part of the Fuka Basin, about 50 m from the tableland, where the elevation ranges from 40 to 70 m above sea level. Finally, it is recommended to drill a group of test wells for performing pumping tests to evaluate a sustainable usage. Also, geophysical studies should be conducted to determine the thickness and the depth of the clay layer as well as the extent of the perched water all over the Fuka Basin.

Acknowledgments Authors are thankful to the DAAD (Deutscher Akademischer Austausch Dienst) and ministry of higher education and scientific research in Egypt who funded the postdoctoral scholarship for the first author, and through which the present research was conducted. Also thanks to the Desert Research Center (Cairo, Egypt), which provided a potential for field studies and the University of Heidelberg (Heidelberg, Germany) for providing all the requirements to conduct research.

Open Access This article is distributed under the terms of the Creative Commons Attribution License which permits any use, distribution and reproduction in any medium, provided the original author(s) and source are credited.

References

- Ali AO, Rashid M, El Naggar S, Abdul Al A (2007) Water harvesting options in the drylands at different spatial scales. *Land Use Water Resour Res* 7:1–13
- American Society of Testing and Materials (ASTM) (2002) Water environmental technology Annual book of ASTM standards, sec. 11.01 and 11.02, West Conshohocken
- Atwa SM (1979) Hydrogeology and hydrogeochemistry of the northwestern coast of Egypt. Ph.D. thesis, Faculty of Science, Alexandria University
- Bubenzer O, Bolten A (2008) The use of new elevation data (SRTM/ ASTER) for the detection and morphometric quantification of Pleistocene megadunes (draa) in the eastern Sahara and the southern Namib. *Geomorphology* 102:221–231
- Collins WD (1923) Graphic representation of analyses. *Ind Eng Chem* 15:394
- Conoco (1986) Geological map of Egypt, scale 1:500,000 GPC, sheet No. NH35NE (Alexandria)
- El-Raey M (1998) Framework of integrated coastal area management of the Fuka-Matrouh area, Egypt, PAP/RAC-37-1995

- El-Raey M, Dewidar KR, El-Hattab M (1999) Adaptation to the impacts of sea level rise in Egypt. *Mitig Adapt Strateg Glob Chang* 4:343–361
- El-Sharabi ES (2000) Hydrogeological, geomorphological and geo-environmental implications for future sustainable development of the northwestern coastal zone of Egypt. Ph.D. Thesis, Mansoura University
- FAO (1970) Pre-investment survey of the northwestern coastal region: physical conditions and water resources. Technical report 2 (ESE: SF/UAR 49)
- Freeze RA, Cherry JA (1979) *Groundwater*. Prentice-Hall, Englewood Cliffs
- Hammad FA (1972) The geology of soils and water resources in the area between Ras El Hekma and Ras El Rum (Western Mediterranean Littoral Zone, Egypt). Ph.D. Thesis, Faculty of Science, Cairo University
- Hefny K, Samir FM, Mohamed H (1992) Groundwater assessment in Egypt. *Int J Water Resour Dev* 8(2):126–134
- IPCC (2007) Climate change: the physical science basis. Contribution of Working Group I to the Fourth Assessment Report of the Intergovernmental Panel on Climate Change. In: Solomon S, Qin D, Manning M, Chen Z, Marquis, Averyt K B, Tignor M and Miller H L (eds) Cambridge University Press, Cambridge
- Kimberley MM, Abu-Jaber N (2005) Shallow perched groundwater, a flux of deep CO₂, and near-surface water–rock interaction in Northeastern Jordan: an example of positive feedback and Darwin's "warm little pond". *Precambr Res* 137:115–292
- Maidment DR (2002) *Arc Hydro, GIS for water resources*. ESRI press, Redlands
- Mohamed TH, Fahmy MM (2005) Carbon dioxide chemistry of the SE Mediterranean open waters off Egypt. *Chem Ecol* 21(1): 37–45
- Moseley F (1973) Desert waters of the Middle East and the role of the Royal Engineers. *R Eng J* 87(3):175–186
- Mudallal UH (1990) Hydrogeological studies of areas in the northwestern coastal zone and Siwa. Project EGY/87/010, FAO, Rome
- Parkhurst DL, Appelo CAJ (1999) User's guide to PHREEQC.: U.S. Geological Survey, Water-Resources Investigations Report 99-4259
- Piper AM (1944) A graphic procedure in the geochemical interpretation of water analyses. *Trans. Am. Geophys*, vol 6. Union, 25, Washington, D.C., pp 914–923
- Robins NS, Rose EP (2009) Military uses of groundwater: a driver of innovation? *Hydrogeol J* 17:1275–1287
- Rose EP (2004) The contribution of geologists to the development of emergency groundwater supplies by the British Army. In: Caldwell RD, Ehlen J, Harmon RS (eds) *Studies in military geography and geology*. Kluwer Academic Publishers, Netherlands, pp 307–319
- Said R (1990) *The geology of Egypt*. Balkema, Rotterdam
- Sailhac P, Bano M, Behaegel M, Girard F, Para EF, Ledo J, Marquis G, Matthey D, Ramirez J (2009) Characterizing the vadose zone and a perched aquifer near the Vosges ridge at the La Soutte experimental site, Obernai, France. *C R Geosci* 341:818–830
- Scholler H (1962) *Les eaux souterraines*. Massio et Cie, Paris
- Sewidan AS (1978) Water Budget analysis for the northwestern coastal zone. Ph.D Thesis, Faculty of Science, Cairo University
- Shaaban FF (2001) Vertical electrical soundings for groundwater investigation in northwestern, Egypt: a case study in a coastal area. *Afr Earth Sci* 33:673–686
- Shata A (1955) An introductory note on the geology of the northern portion of the Western Desert of Egypt. *Bull Inst Desert* 5(2):96–106
- Shata A (1957) Geology and geomorphology of Wadi El Kharrupa area, vol 10. Publ. inst. Desert, Egypt, pp 91–120
- Sherif MM, Singh VP (1999) Effect of climate change on sea water intrusion in coastal aquifers. *Hydrol Process* 13:1277–1287
- Shotton FW (1944) The Fuka Basin. *R Eng J* 58(2):107–109
- Underwood J, Guth P (1998) *Military geology in war and peace*. GSA, Boulder, p 245
- Worsley R (1939) The hydrogen ion of Egyptian soil. Ministry of Agriculture, Egypt Bull. No. 83, pp 1–33
- Wu YS, Ritcey AC, Bodvarsson GS (1999) A modeling study of perched water phenomena in the unsaturated zone at Yucca Mountain. *J Contam Hydrol* 38:157–184
- Zaporozec A (1972) Graphical interpretation of water quality data. *Groundwater* 10(2):32–43